Low-energy surface phonons on α-quartz (0001)

W. Steurer,* A. Apfolter, M. Koch, W. E. Ernst, and B. Holst†
Institute of Experimental Physics, Graz University of Technology, 8010 Graz, Austria

E. Søndergård
Laboratoire Surface du Verre et Interfaces, CNRS/Saint-Gobain, UMR 125, 39 Quai Lucien Lefranc, 93303 Aubervilliers Cedex, France

S. C. Parker
Department of Chemistry, University of Bath, Bath BA2 7AY, United Kingdom

(Received 17 January 2008; revised manuscript received 2 June 2008; published 1 July 2008)

Calculated surface-phonon-dispersion curves for a dry, a partly hydroxylated, and a fully hydroxylated α-quartz (0001) surface are presented and compared with first low-energy inelastic helium-atom scattering measurements. Qualitative agreement between the calculations and the observed Rayleigh-wave dispersion curve is achieved for the dry quartz surface. A signature effect is seen in the calculated phonon-dispersion curves for the fully hydroxylated surface.

DOI: 10.1103/PhysRevB.78.035402 PACS number(s): 72.10.Di, 42.70.Ce, 68.49.Bc

I. INTRODUCTION

Although quartz surfaces are of paramount importance in a variety of technical applications, experimental structural information about the α-quartz surface is sparse. Several surface-sensitive techniques, which are routinely used to investigate conducting surfaces, are rendered unfeasible due to the insulating nature of silica. Nonetheless, experimental investigations of the α-quartz surface have been conducted using atom force microscopy (AFM)[1,2] and low-energy-electron diffraction (LEED).[3,4] However, no detailed structural information was obtained. Helium-atom scattering (HAS) can provide information at the atomic scale and has proven to be ideally suited for unveiling the quartz surface structure.[5] The very first HAS spectra have confirmed the (1×1) pattern previously observed in LEED studies and have unveiled additional weak (2×2) peaks.[5] The experimental results were found to be in good agreement with the theoretically predicted reconstruction of the dry α-quartz surface by de Leeuw *et al.*[6] and Rignanese *et al.*[7] In order to account for the observed symmetries in the HAS spectra, however, a model has been proposed in which terraces with step heights that are multiples of 1/3 of the unit-cell height lead to domains rotated by $\pm60°$ relative to each other. An experimental investigation of the surface dynamics of α-quartz by HAS has been reported recently.[8] Thermal attenuation measurements of scattered helium atoms have yielded a value of 0.011 nm for the vibration amplitude at room temperature as well as a first estimate of the surface Debye temperature, $\Theta_D=360$ K.

A number of atomistic simulations have been performed the last few years to compensate for the chronic lack of detailed experimental data. These have included both density-functional theory (DFT) and interatomic-potential approaches for evaluating the forces on the atoms. Using both methodologies, simulations by Rignanese *et al.*[7] and de Leeuw *et al.*[6] have calculated the same surface reconstruction. A recent reinvestigation using a hybrid DFT functional has confirmed the predicted structures in both dry and wet conditions[9] and has begun to explore the surface reactivity. The strength of such DFT methods is that they can model chemical reactivity and evaluate the change in the surface structure with different external conditions, thereby allowing the surface phase diagram[10] to be predicted. However, these methods still require a large amount of computer time and make it difficult to investigate the properties of large numbers of atoms. In contrast, interatomic-potential approaches can explore the effect of dynamics and system size. Du and de Leeuw[11] recently modeled the water-quartz interface using molecular dynamics. Thus, at the present time, interatomic-potential approaches are the most efficient choice for probing the dynamics for large numbers of atoms.

Here we present atomistic simulations of surface-phonon-dispersion curves for the surface of α-quartz (0001) and compare them with low-energy HAS measurements. Calculations are performed for a dry surface without hydroxyl groups,[6,7,9] a partly hydroxylated surface with vicinal OH groups, and a fully hydroxylated surface with geminal OH groups. These surface reconstructions (see Fig. 1) are of great interest since the dry one corresponds to the initial state after sample preparation, the hydroxylated surface is known to be the most stable one, and the partially hydroxylated surface describes an intermediate state. Water molecules will be present even under ultrahigh-vacuum (UHV) conditions and will be adsorbed by the hydrophilic dry surface.[12] Depending on the partial pressure of water in the UHV chamber, it is expected that with time the quartz surface gradually changes its surface structure. Our simulations show different behavior of the surface-phonon-dispersion curves for the three investigated surfaces. A signature effect is predicted for the $\bar{K}-\bar{M}$ orientation between the dry and the fully hydroxylated surface. This effect suggests surface-phonon measurements by HAS as a method for determining the amount of OH groups on crystalline silica surfaces. The Rayleigh-wave dispersion curve is clearly observed in the experimental HAS results. Qualitative agreement between simulations and measurements is achieved for the dry surface.

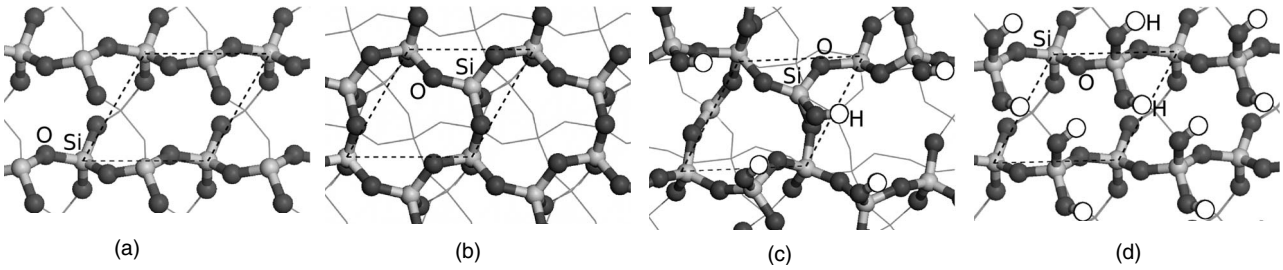

FIG. 1. Projection of (a) cleaved, (b) reconstructed, (c) partly hydroxylated, and (d) fully hydroxylated quartz surfaces onto the (0001) plane. Under dry conditions, i.e., no water being present, the cleaved quartz (0001) surface (a) relaxes to form the "bridge structure" (Refs. 6, 7, and 9) (b) with a reduced surface energy of 1.48 J/m^2 compared to 4.0 J/m^2 for the cleaved surface. Further reduction in the surface energy will occur in a wet environment with a surface energy of 0.38 J/m^2 for the fully hydroxylated surface (d). The partly hydroxylated surface is only of hypothetical use since it results in an increased surface energy of 3.75 J/m^2. (c) NB: Only the topmost layer of atoms is shown. The surface unit cell is indicated by dashed lines in all figures; sketched lines in the background represent the bulk structure.

II. CALCULATIONAL DETAILS

We used the minimum energy technique applied to dislocation, interface and surface energies (METADISE) (Ref. 13) for generating slabs of different thicknesses ranging from 3 to 6 nm. The structures for the (0001) quartz surfaces when dry and fully hydroxylated were described previously[6] and were later confirmed by electronic structure simulations.[7,9] The vibrational frequencies (phonons) were generated using the lattice-dynamics treatment of solids.[14] The normal modes were assumed to be harmonic. The solution of the equations of motion leads to a simple eigenvector equation from which the vibrational frequencies can be extracted. The only issue is that the periodic nature of the solid must be taken into account by including the dependence of the displacements and second derivatives on the wave vector, k. This approach is coded in phonon assisted relaxation applied to the prediction of crystal structures (PARAPOCS),[15] which has been used successfully for silicates. Predicting the thermal contraction of siliceous zeolites[16] and identifying mode softening in the high-pressure amorphization transition in quartz[17] are just two examples to be mentioned. The quality of three interatomic potentials was investigated for quartz by comparison of thermodynamic, vibrational, elastic, and structural properties as a function of temperature and pressure with experiment.[18] It was found that the vibrational dispersion curves were best modeled by the shell-model potential of Sanders *et al.*[19] Thus, given the good agreement of both surface structure and phonon frequencies, we used this potential along with the modifications for the hydroxylated surface.[20] This potential is characterized by the use of full valence charges for silicon with two and three body short-range contributions. The polarizability is modeled by assigning core and shell positions connected by a harmonic spring to each oxygen atom.

III. EXPERIMENTAL SETUP

For the experiments presented here, a Z-cut polished and twin-free $10\times10\times1$ mm^3 α-quartz sample was used. The sample was first cleaned in a soap solution and then annealed to 1025° for 72 h under a pressure of 2 bar of oxygen in order to eliminate residual scratches from the polishing process. The long annealing time also assures that the investigated sample is free of hydroxyl groups. AFM images of the sample, which were obtained right after the annealing treatment, show steps and/or terraces with a terrace length of 200 nm and a high number of defect sites, such as pit holes.[5] The cleaned sample was then transferred to the helium scattering apparatus[21] in Graz using a transport container under an argon atmosphere. Before starting experiments the surface was exposed to an initial cleaning *in situ*. The cleaning was carried out by heating the sample to about 370 °C for 2 h under a high partial pressure of O_2 to burn away carbon contaminates. The experiments were all carried out with a base pressure in the 10^{-9} mbar range. For a detailed description of the cleaning procedure we refer to a previous publication.[5] For the HAS experiments a monochromatic beam was created by supersonic expansion through a 10 μm nozzle. The central part of the beam was selected using a 400 μm skimmer. The beam energy was 22.0 meV with a spread of $\delta E/E \approx 2\%$ for all experiments. The scattered helium atoms were measured using a magnetic-sector mass spectrometer mounted 1618 mm from the sample surface. The scattering angle was kept fixed at 90°, and the crystal was rotated in the scattering plane (the plane containing the incident beam, the surface normal, and the final beam), with incident angles between 29.6° and 49.6° (see Fig. 2). The reflectivity of the surface was found to be very low, presumably because of the beforementioned high number of defect sites on the surface. The thus required very long recording times of 10 000 s per spectrum put a constraint on the number of spectra that could be measured. In order to assure stable conditions during the long recording times and to prevent water molecules from condensating on the surface, all experiments were performed with the sample at room temperature. All time-of-flight (TOF) plots presented herein are converted to the energy-transfer scale for the abscissa and to the differential reflection coefficient for the ordinate, respectively. TOF data were obtained at a bin width of 5 μs.

IV. RESULTS AND DISCUSSION

For the sake of preparing a framework for a meaningful discussion of the calculated phonon curves, experimental results are presented first. In Fig. 2, time-of-flight measure-

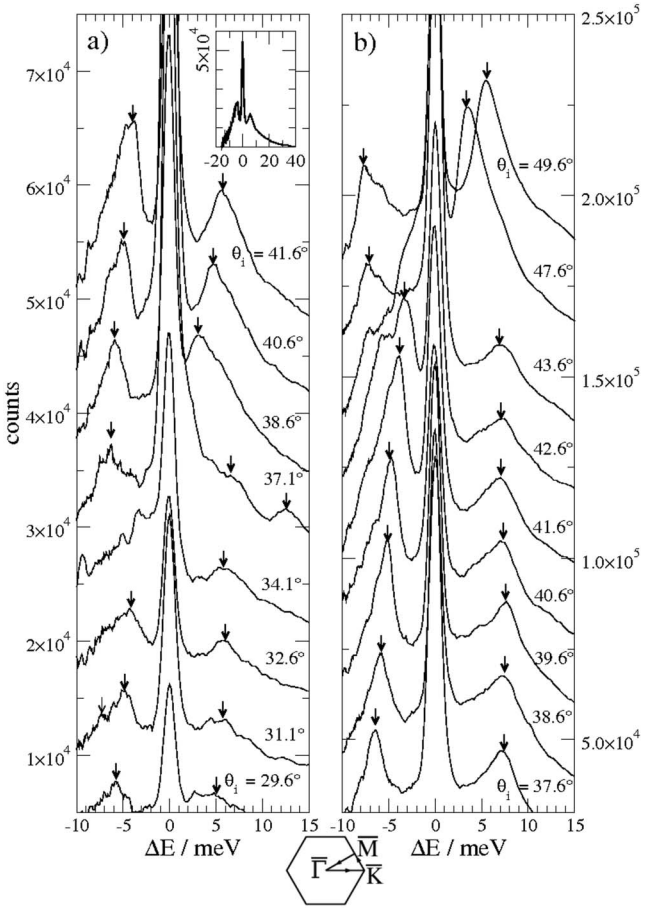

FIG. 2. Measured time-of-flight spectra for different incident angles along the (a) $\bar{\Gamma}-\bar{M}$ and (b) $\bar{\Gamma}-\bar{K}$ azimuths. The spectra have been converted from flight time to energy-transfer scale. The incident energy was 22.0 ± 0.2 m eV, and the surface temperature was $T_s=300$ K. The bold arrows mark strong phonon peaks. In addition to the diffuse elastic peak at $\Delta E=0$, a dispersive surface phonon and an Einstein-type mode at ≈ 6 m eV can be clearly seen. For sake of clarity the spectra are vertically offset by 2000 counts (a) and 600 counts (b), respectively. A representative spectrum (corresponding to $\theta_i=41.6°$) is shown in full scale in the inset.

ments are presented in an energy-transfer scale along the $\bar{\Gamma}-\bar{M}$ and $\bar{\Gamma}-\bar{K}$ azimuths. Each curve shows, at $\Delta E=0$ meV, an elastic-scattered peak on top of a quite intense multiphonon background, as can be seen from the inset of Fig. 2. The elastic peak is attributed to diffuse scattering from structural defects. The predominance of the elastic peak gives further evidence that the density of defect sites was very high on the investigated sample. The phonon peaks (indicated by arrows) are seen in addition to the elastic peak on the phonon creation ($\Delta E<0$) and annihilation sides ($\Delta E>0$).

The presence of the multiphonon background further hampers the extraction of the phonon peaks. The low surface Debye temperature $\Theta_D=360$ K (Ref. 8) and the small effective mass of the surface, $M_{\text{surface}}=20$ a.u.,[8] make it difficult to obtain data without a deleterious effect from a multiphonon background. This can be understood from the Weare criterion,[22]

$$\beta=\frac{M_{\text{beam}}}{M_{\text{surface}}}\frac{(E_{iz}+D)T_S}{k_B\Theta_D^2}\leq 0.01, \tag{1}$$

where M_{beam} is the projectile mass, E_{iz} is the perpendicular incident energy, D is the well depth, and T_S is the surface temperature. In order to assure a good signal without a large multiphonon background, β should be close to 0.01. With the values for Θ_D and M_{surface} from above and $D=9.7$ meV,[23] $\beta=0.11$ in the present experiments, thus indicating a large multiphonon background. Since the smallest possible energy E_i of the scattering apparatus was already chosen, further decrease in β could only be achieved by choosing a lower surface temperature. However, since a smaller temperature also reduces the density of phonon states,[24] no net effect results from measuring at a lower temperature.

The energy and parallel momentum transfer of all measured phonon peaks are summarized in the extended zone diagram of Fig. 3 for both measured surface orientations. Experimental scan curves showing the geometrically allowed parallel momentum transfers (ΔK) corresponding to the energy transfer (ΔE) are plotted as dashed lines.

Atomistic simulations of the α-quartz (0001) surface-phonon-dispersion curves were performed for three different surface reconstructions. In Fig. 4, calculated surface-phonon spectra are shown for a dry, a partly hydroxylated, and a fully hydroxylated quartz surface, together with the experimental data from Fig. 2, folded into the irreducible part of the first Brillouin zone. A number of four to five surface-

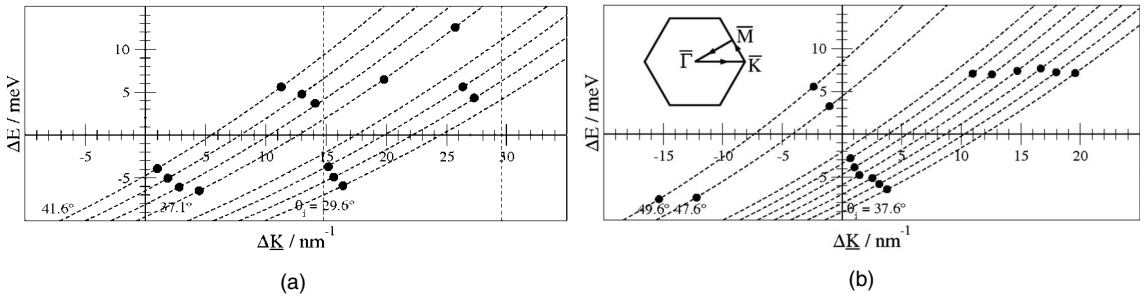

FIG. 3. Measured dispersion curves in an extended zone scheme for the two directions: (a) $\bar{\Gamma}-\bar{M}$, reciprocal-lattice vector $G=14.8$ nm^{-1} and (b) $\bar{\Gamma}-\bar{K}$, $G=25.63$ nm^{-1}. The dashed lines show the scan curves at the indicated incident angles. The filled circles (●) correspond to the peaks marked by arrows in the measured TOF spectra from Fig. 2. $\Delta E>0$ corresponds to annihilation and $\Delta E<0$ to creation events.

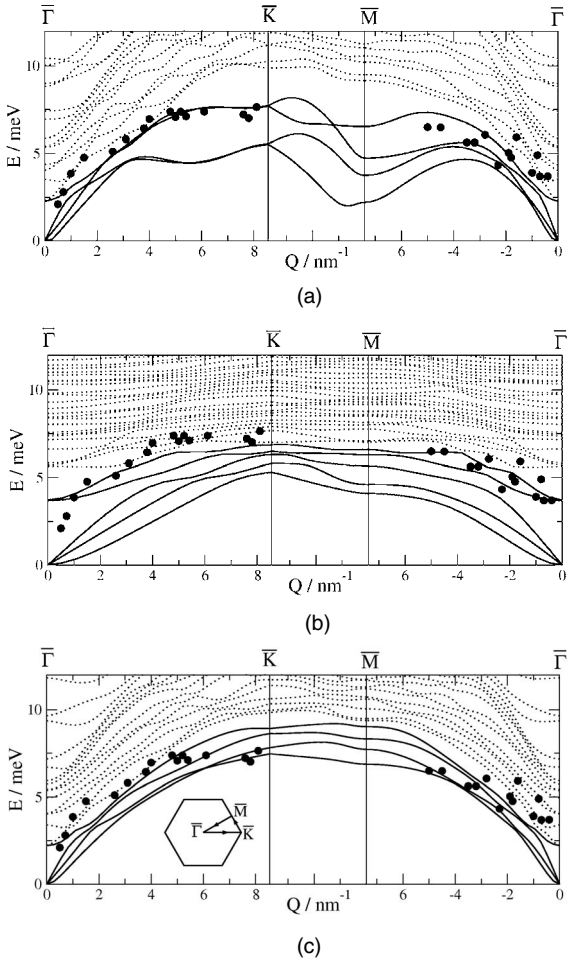

FIG. 4. Calculated phonon-dispersion curves as a function of the surface wave vector Q along the boundary $\bar{\Gamma}\rightarrow\bar{K}\rightarrow\bar{M}\rightarrow\bar{\Gamma}$ of the irreducible part of the first surface Brillouin zone for a dry (0001) surface showing the "bridge"-reconstruction (a), partly hydroxylated (b), and a fully hydroxylated (0001) surface (c). The zone-boundary vectors are $\bar{\Gamma}-\bar{K}=8.54$ nm^{-1}, $\bar{\Gamma}-\bar{M}=7.4$ nm^{-1}, and $\bar{K}-\bar{M}=3.7$ nm^{-1}. Four surface-localized modes detached from the bulk continuum (dotted lines) are clearly discernible (five in case of the partly hydroxylated surface, respectively). The calculated slab was of thickness of 3.4 nm (60 layers). The distinct experimental data points from Fig. 3 are shown for comparison (●). The calculated slabs had a thickness of 3.5 nm (60 layers).

localized modes detached from the bulk continuum are clearly discernible in all depictions. The calculated surface-localized phonon curves show an apparent dependence on the presence of OH groups at the surface. Most noticeably, the zone-boundary energies at the $\bar{M}$ and $\bar{K}$ points increase with increasing OH concentrations. Furthermore, a strong signature effect is predicted between the dry and the fully hydroxylated surface along the $\bar{K}-\bar{M}$ direction. However, since inelastic HAS experiments along $\bar{K}-\bar{M}$ are much more sophisticated than measuring along principal directions, data points were only obtained along $\bar{\Gamma}-\bar{K}$ and $\bar{\Gamma}-\bar{M}$ in this first HAS investigation. Qualitative agreement between the experimental data points and the calculated phonon curves is achieved for the dry surface (see Fig. 4). Especially along $\bar{\Gamma}-\bar{K}$ the experimental data points coincide with a calculated phonon mode for the dry surface, an agreement that is not seen for the other surface realizations. We do not see any of the low-energy points expected for the dry surface along $\bar{\Gamma}-\bar{K}$ however. This cannot satisfactorily be explained yet and requires further investigations. Indications that hydrolysis of the sample during the experiment was not a relevant process, coming also from the fact that the sample surface retained a constant He reflectivity over several days. If hydrolysis had taken place to a significant extent, then the OH groups would have acted as point defects that would have lowered the intensity over time.

V. CONCLUSIONS

In conclusion, we have presented an investigation of low-energy surface-phonon-dispersion curves of α-quartz (0001) by a combined approach of atomistic simulations and first experimental HAS data. Simulations for the dry surface and the fully hydroxylated surface with geminal OH groups unveil different phonon behaviors. A predicted signature effect along the $\bar{K}-\bar{M}$ direction suggests HAS as a sensitive probe for determining OH concentrations at crystalline silica surfaces. The best agreement between the experimental data points and calculated surface-phonon-dispersion curves is achieved for the dry quartz surface, indicating that the sample surface is almost free of OH bonds. The study presented here gives impetus to a meticulous investigation of the quartz surface dynamics on both dry and hydroxylated surfaces and opens for new applications of HAS.

ACKNOWLEDGMENTS

The authors thank C. Arrouvel and W. Greń for assistance with the simulations. The authors also thank J. R. Manson for many stimulating discussions. One of us (W.S.) is thankful to the University of Bath for their hospitality while working on the simulations and to the Austrian Academy of Science for a DOC Grant. The authors gratefully acknowledge support from the European Commission, FP6, NEST STREP ADVENTURE program, Project INA, Contract No. 509014.

*wolfram.steurer@gmail.com
†Present address: Department of Physics and Technology, University of Bergen, Allegaten 55, 5007 Bergen, Norway.

[1] A. J. Gratz, S. Manne, and P. K. Hansma, Science **251**, 1343 (1991).
[2] M. Kawasaki, K. Onuma, and I. Sunagawa, J. Cryst. Growth **258**, 188 (2003).
[3] I. Janossy and M. Menyhard, Surf. Sci. **25**, 647 (1971).
[4] F. Bart and M. Gautier, Surf. Sci. **311**, L671 (1994).
[5] W. Steurer, A. Apfolter, M. Koch, T. Sarlat, E. Søndergård, W. Ernst, and B. Holst, Surf. Sci. **601**, 4407 (2007).
[6] N. de Leeuw, F. Higgins, and S. Parker, J. Phys. Chem. B **103**, 1270 (1999).
[7] G. M. Rignanese, A. De Vita, J. C. Charlier, X. Gonze, and R. Car, Phys. Rev. B **61**, 13250 (2000).
[8] W. Steurer, A. Apfolter, M. Koch, W. E. Ernst, and B. Holst, Surf. Sci. **602**, 1080 (2008).
[9] T. P. M. Goumans, A. Wander, W. A. Brown, and C. R. A. Catlo, Phys. Chem. Chem. Phys. **9**, 2146 (2007).
[10] E. Chagarov, A. A. Demkov, and J. B. Adams, Phys. Rev. B **71**, 075417 (2005).
[11] Z. Du and N. H. de Leeuw, Dalton Trans. 22, 2623 (2006).
[12] The hydrophilicity is best seen in the greatly reduced surface energy of the hydroxylated surface compared to the dry surface.
[13] G. W. Watson, E. T. Kelsey, N. H. de Leeuw, D. J. Harris, and S. C. Parker, J. Chem. Soc., Faraday Trans. **92**, 433 (1996).
[14] M. Born and K. Huang, *Dynamical Theory of Crystal Lattices* (Oxford University Press, New York, 1954).
[15] S. Parker and G. Price, Adv. in Solid-State Chem. **1**, 295 (1989).
[16] P. Tschaufeser and S. C. Parker, J. Phys. Chem. **99**, 10609 (1995).
[17] G. W. Watson and S. C. Parker, Phys. Rev. B **52**, 13306 (1995).
[18] K. de Boer, A. P. J. Jansen, R. A. van Santen, G. W. Watson, and S. C. Parker, Phys. Rev. B **54**, 826 (1996).
[19] M. Sanders, M. Leslie, and C. R. A. Catlow, J. Chem. Soc., Chem. Commun. **1984**, 1271.
[20] P. Baram and S. C. Parker, Philos. Mag. B **73**, 49 (1996).
[21] A. Apfolter, M.S. thesis, Graz University of Technology, 2005.
[22] J. H. Weare, J. Chem. Phys. **61**, 2900 (1974).
[23] V. Druzhinina and M. DeKieviet, Phys. Rev. Lett. **91**, 193202 (2003).
[24] J. P. Toennies, in *Surface Phonons*, edited by W. Kress and F. W. De Wette (Springer, Berlin, 1991).